International Journal of Pharmaceutics 403 (2011) 192–200

Contents lists available at ScienceDirect

International Journal of Pharmaceutics

journal homepage: www.elsevier.com/locate/ijpharm

Pharmaceutical Nanotechnology

Nano spray drying: A novel method for preparing protein nanoparticles for protein therapy

Sie Huey Lee [a], Desmond Heng [a,*], Wai Kiong Ng [a], Hak-Kim Chan [b], Reginald B.H. Tan [a,c,**]

[a] Institute of Chemical and Engineering Sciences, A*STAR (Agency for Science, Technology and Research), 1, Pesek Road, Jurong Island, Singapore 627833, Singapore
[b] Advanced Drug Delivery Group, Faculty of Pharmacy, A15, The University of Sydney, Sydney, NSW 2006, Australia
[c] Department of Chemical and Biomolecular Engineering, National University of Singapore, 4 Engineering Drive 4, Singapore 117576, Singapore

ARTICLE INFO

Article history:
Received 30 July 2010
Received in revised form 3 October 2010
Accepted 7 October 2010
Available online 15 October 2010

Keywords:
Nano spray dryer
Protein therapy
Nanoparticles
Bovine serum albumin
Spray drying

ABSTRACT

There has been an increasing interest in the development of protein nanotherapeutics for diseases such as cancer, diabetes and asthma. Spray drying with prior micro mixing is commonly used to obtain these powders. However, the separation and collection of protein nanoparticles with conventional spray dryer setups has been known to be extremely challenging due to its typical low collection efficiency for fine particles less than 2 μm. To date, there has been no feasible approach to produce these protein nanoparticles in a single step and with high yield (>70%). In this study, we explored the feasibility of the novel Nano Spray Dryer B-90 (equipped with a vibrating mesh spray technology and an electrostatic particle collector) for the production of bovine serum albumin (BSA) nanoparticles. A statistical experimental design method (Taguchi method based on three levels, five variables L_{18} orthogonal array robust design) was implemented to study the effect of and optimize the experimental conditions of: (1) spray mesh size, (2) BSA solution concentration, (3) surfactant concentration, (4) drying air flow rate and (5) inlet temperature on: (1) size and (2) morphology (axial ratio). Particle size and morphology were predominantly influenced by the spray mesh size and surfactant concentration, respectively. The drying air flow rate and inlet temperature had minimal impact. Optimized production of smooth spherical nanoparticles (median size: 460 ± 10 nm, axial ratio: 1.03 ± 0.00, span 1.03 ± 0.03, yield: 72 ± 4%) was achieved using the 4 μm spray mesh at BSA concentration of 0.1% (w/v), surfactant concentration of 0.05% (w/v), drying flow rate of 150 L/min and inlet temperature of 120 °C. The Nano Spray Dryer B-90 thus offers a new, simple and alternative approach for the production of protein nanoparticles suited for a variety of drug delivery applications.

1. Introduction

Although protein therapy has been around for a number of years, it is still an important and evolving area of research in view of the current clinical delivery limitations and the increasing emphasis placed on vaccines, hormones, growth factors, monoclonal antibodies and enzymes to treat the wide array of diseases afflicting the human population (Larry, 2005).

Therapeutic proteins are hardly administered orally due to their low oral bioavailability as a result of enzymatic degradation, poor membrane permeability and short physiological half-lives in the gastric and intestinal fluids (Lee et al., 2007; Shaji and Patole, 2008). These drugs are rapidly cleared before successful tissue penetration. Therefore, the parenteral route is still the standard delivery option for current and emerging biopharmaceuticals.

However, the quest to improve patient compliance has fuelled development into alternative non-invasive delivery options such as controlled peroral delivery, pulmonary delivery, nasal delivery and transdermal delivery (Cleland et al., 2001). As some of these alternative delivery methods involve formulation in the dry powdered form, formulation strategies (e.g. size, morphology) thus have to be re-developed and optimized for the specific delivery system.

Spray drying is a well-established method commonly used in the pharmaceutical industry for producing a dry powder from a liquid phase (Broadhead et al., 1992). In recent years, it has been identified as a suitable method for the preparation of proteins intended for pulmonary (Chan et al., 1997; Salama et al., 2009), nasal (Kaye et al., 2009) and controlled oral delivery (Coppi et al., 2002). It offers the advantage of drying and particle formation in a single-step continuous and scalable process with particle engineering possibilities

* Corresponding author. Tel.: +65 67963861; fax: +65 63166183.
** Corresponding author at: Institute of Chemical and Engineering Sciences, A*STAR (Agency for Science, Technology and Research), 1, Pesek Road, Jurong Island, Singapore 627833, Singapore. Tel.: +65 67963855; fax: +65 63166183.
E-mail addresses: desmond_heng@ices.a-star.edu.sg (D. Heng), reginald_tan@ices.a-star.edu.sg (R.B.H. Tan).

0378-5173/$ – see front matter © 2010 Elsevier B.V. All rights reserved.
doi:10.1016/j.ijpharm.2010.10.012

(Masters, 1976). Furthermore, various particle properties such as particle size, bulk density and flow properties can easily be tuned via simple manipulation of the process parameters or spray dryer configuration. Therefore, spray drying is potentially a versatile and commercially viable technique for formulating protein and peptide drugs.

The typical spray drying process encompasses four fundamental steps: (a) atomization of feed into a spray, (b) spray–air contact, (c) drying of spray, and (d) separation of dried product from the drying air (Masters, 1976). A liquid feedstock is atomized into a spray of fine droplets and then brought into contact with the hot drying gas at sufficient temperature for the moisture evaporation to take place. As the moisture evaporates from the droplets, the solid product is formed, and the powder is readily recovered from the drying gas. The field of spray drying is constantly evolving. Since the first development of spray drying technology in the early 1870s (Cal and Sollohub, 2010), there have been numerous efforts undertaken to refine the equipment and technology to ensure relevance and attractiveness to the food and pharmaceutical industry.

As nanotechnology is increasingly finding niche applications in drug delivery, many pharmaceutical companies are hence enthusiastically embracing nanoparticles into their formulations. The definition of a nanoparticle depends on the discipline and in the pharmaceutical industry, it is commonly described as having a size between a few nanometers to 1 μm (Heng et al., 2008; Muller and Junghanns, 2006).

In drug delivery, nanoparticles are favored over microparticles due to their small size and higher specific surface area which favorably results in much improved dissolution rates and bioavailabilities (Heng et al., 2008; Noyes and Whitney, 1897). Its other benefits include dose minimization/toxicity reduction, and improved drug penetration (Koster et al., 1996; Souto and Muller, 2008).

During the early stage development of a drug candidate, where the samples are available only in small amounts and are usually expensive, it would be highly beneficial if a formulation could be prepared and studied on a much smaller scale. Therefore, a spray dryer capable of generating nanoparticles directly from solution in a single step and on a much reduced scale would be highly novel and valuable at the research and development stage. The applications of peptide nanostructures have previously been demonstrated in tissue engineering (Ellis-Behnke et al., 2006) and in the development of antibacterial agents (Ghadiri et al., 1994). Furthermore, insulin nanoparticles had also been identified to be a suitable formulation approach for poorly water soluble Zn-insulin (Merisko-Liversidge et al., 2004).

More recently, Buchi® has introduced a new generation (i.e. 4th generation) of laboratory scale spray dryer that is able to generate particles in the size range of 300 nm to 5 μm for milligram sample quantities at high yields (BÜCHI Labortechnik AG, 2009; Schmid et al., 2010). As the desired particle size of most drug delivery applications in the oral, intravenous, transdermal and pulmonary fields fall within this size range, the appeal of this spray dryer to the drug delivery community would indeed be significant (Chiou et al., 2008; Heng et al., 2009; Koster et al., 1996; Souto and Muller, 2008).

The novel technologies at the spray head, heating system and particle collector of the Nano Spray Dryer B-90 have made 'nano' spray drying a possibility. Unlike conventional spray dryers that use rotary atomizers (atomization by centrifugal energy) and pressure nozzles (atomization by pressure energy) or two-fluid nozzle (atomization by kinetic energy) for forming the spray droplets, the new Nano Spray Dryer B-90 utilizes a vibrating mesh technology for fine droplets generation. Basically, the piezoelectric crystal driven spray head is incorporated with a small spray cap that contains a thin perforated membrane (spray mesh) having an array of precise micron-sized holes (i.e. spray meshes of 4 μm, 5.5 μm or 7 μm hole size). When the piezoelectric actuator is driven at an ultrasonic frequency (i.e. 60 kHz), the mesh will vibrate upwards and downwards, injecting millions of precisely sized droplets from the holes and generating the aerosols. Fig. 1 illustrates the functional principle of mesh vibration occurring at the piezoelectric driven spray head of the Nano Spray Dryer B-90.

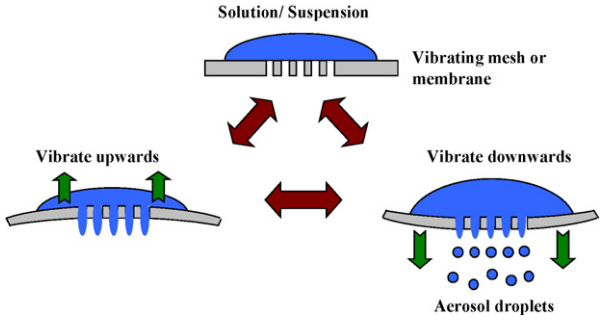

Fig. 1. The functional principle of mesh vibration occurring at the piezoelectric driven spray head of the Nano Spray Dryer B-90, adapted by permission from BÜCHI Labortechnik AG (2009), Flawil, Switzerland.

Although turbulent flow in a spray dryer promotes more efficient drying as a result of higher heat transfer efficiency, exposure of the particles to elevated temperatures can sometimes result in a loss of activity for heat-sensitive materials. Favorably, the heating system of the Nano Spray Dryer B-90 operates on a laminar flow principle, whereby the laminar flow is generated by air passing through a compact porous metal foam that is conducive for optimal energy input and has short heating-up rates. With laminar flow, gentle heating is achievable, thus making the system extremely ideal for heat-sensitive biopharmaceutical products. Furthermore, the vertical configuration of the spray dryer facilitates direct and straight-down collection of the particles into the collector, which helps to minimize particle adherence to the side walls of the glass chamber, and hence allowing for much higher collection yields.

In contrast to the common cyclone technology where particles smaller than 2 μm are typically not captured (Mosen et al., 2004), particle separation in the Nano Spray Dryer B-90 involves the use of the electrostatic precipitator whereby the collection mechanism is independent of particle mass. Collection of fine particles with high efficiency is achieved with the novel electrostatic particle collector consisting of a grounded star electrode (cathode) and cylindrical particle collecting electrode (anode). The presence of a high voltage around the particle collector creates an electrostatic field that accelerates the deposition of negatively charged particle onto the inner wall of particle collecting electrode. This is followed by a discharging process. Fig. 2 illustrates the functional principle of an electrostatic particle collector in the Nano Spray Dryer B-90.

As the fields of biotechnology and nanotechnology increasingly overlap and mature, more emphasis will be placed on protein nanotherapeutics and their associated development. Suitable production methods have to be established to meet the demands of this novel hybrid field. In this work, the novel Nano Spray Dryer B-90 was used to investigate the effects of various spray drying process (spray mesh size, nitrogen flow rate and inlet temperature) and formulation parameters (solute solution concentration and surfactant concentration) on the particle characteristics (i.e. particle size and particle morphology) of a protein. Bovine serum albumin (BSA) was used as the model protein. To the best of the authors' knowledge, the use of this novel spray dryer for the production of protein nanoparticles have not been thoroughly examined. Therefore, the aims of this work are to study and optimize the production of protein nanotherapeutics via the novel Nano Spray Dryer B-90.

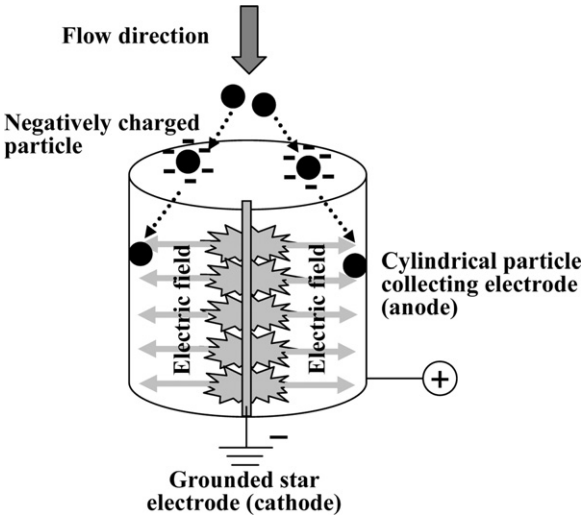

Fig. 2. The functional principle of an electrostatic particle collector in the Nano Spray Dryer B-90.

2. Materials and methods

2.1. Materials

Bovine serum albumin (BSA), fraction V and polyoxyethylene sorbitan monooleate (Tween 80) were supplied by Sigma Chemical Co. (Louis, MO, USA). Ultrapure water was used in the experiments.

2.2. Experimental design

To effectively tune the size and morphology of these protein nanoparticles, a number of process and formulation factors have to be considered. Due to the complexities (i.e. parameter interactions) and the large number of factors involved, optimizing these parameters via conventional optimization protocols (e.g. factorial designs) would be deemed highly laborious and inefficient (Heng et al., 2009). The Taguchi method, being highly applicable for the study of a large number of factors and interactions within a reasonable number of trials (Diemunsch et al., 1993; Kim et al., 2007) was applied in this work to study the effects of various formulation and process factors on the size and morphology of protein nanoparticles. This method is a combination of mathematical and statistical techniques incorporated into an empirical study (Kim et al., 2007) and has previously been applied to the development of pharmaceuticals (Diemunsch et al., 1993; Heng et al., 2009; Palmieri and Wehrle, 1997) The series of established trials aimed to determine the optimum combination of parameters that have the greatest influence on the performance and with the least variation from the design target (Yang et al., 2007).

The Taguchi design method was applied in this study to identify the dominant factors affecting the size and morphology of spray-dried BSA nanoparticles. Three process parameters (spray mesh size, nitrogen flow rate and inlet temperature) and two formulation parameters (protein concentration and surfactant concentration) were evaluated, each at three levels (Table 1) – L_{18} orthogonal array. Optimum conditions were indicated by high signal-to-noise (S/N) ratios. Optimization of both the size and morphology (i.e. axial ratio) was carried out using the Taguchi's 'smaller-is-better' criterion (Eq. (1)) (Peace, 1993; Taguchi, 1986).

Minimize performance characteristic ("smaller-is-better"):

$$(S/N)_i = -10 \cdot \log_{10}\left[\sum_{i=1}^{n} \frac{y_i^2}{n}\right] \quad (1)$$

Table 1
Experimental parameters (factors) and levels.

Parameters	Levels		
	1	2	3
(A) Spray mesh (μm)	4	5.5	7
(B) Surfactant (Tween 80) concentration (%, w/v)	0	0.05	0.5
(C) Protein (BSA) concentration (%, w/v)	0.5	1	2
(D) Nitrogen flow rate (L/min)	90	120	150
(E) Inlet temperature (°C)	80	100	120

where y_i is the characteristic property and n is the number of experimental replicates.

2.3. Spray drying

All formulations in the study were prepared via spray drying on the Nano Spray Dryer B-90 (BÜCHI Labortechnik AG, Flawil, Switzerland). Fig. 3 shows the schematic diagram of the spray drying process. Aqueous solutions of BSA and Tween 80 (surfactant) of various concentrations were dissolved in ultrapure water and then spray-dried at a range of experimental conditions (Table 1). All solutions were filtered through a 0.45 μm syringe filter (Millipore, Bedford, MA, USA) prior to spray-drying to minimize blockage due to any undissolved particles at the spray mesh. The resulting outlet temperature, under aforementioned conditions, varied between 36 and 55 °C. The dried powder was collected from the particle collecting electrode using a particle scraper and then stored in a desiccator at room temperature for further characterization.

2.4. Surface morphology, geometric size and morphology of particle

The surface morphology of the spray-dried BSA particles was observed by a field emission scanning electron microscope (FESEM, JEOL JSM-6700). Prior to imaging, the samples were dispersed onto carbon sticky tabs and coated with gold for 80 s. The particle size

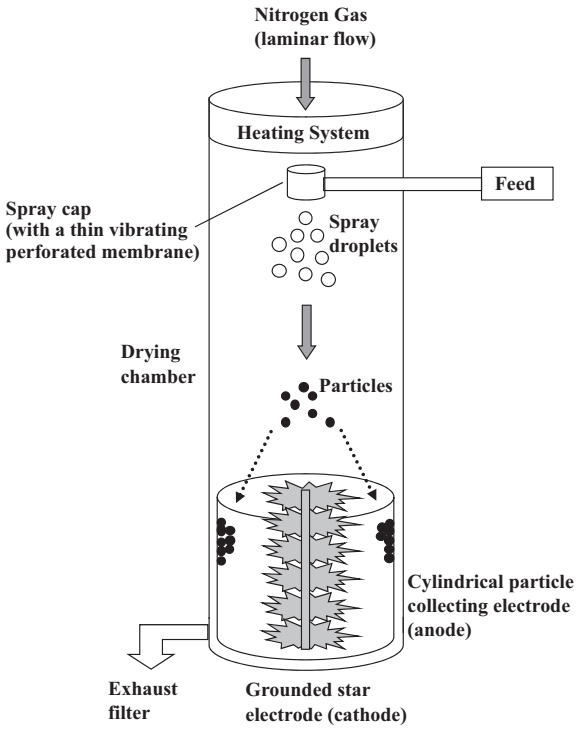

Fig. 3. Schematic diagram of the laboratory-scale Nano Spray Dryer B-90.

Table 2
Experimentally measured values and their corresponding S/N ratios for the response variables.

Run	Parameters					Particle size (nm)		Axial ratio	
	A	B	C	D	E	y (n = 3)	S/N ratio (dB)	y (n = 3)	S/N ratio (dB)
1	1	1	1	1	1	785 (51)	−57.9	1.34 (0.02)	−2.54
2	1	2	2	2	2	733 (68)	−57.3	1.01 (0.00)	−0.11
3	1	3	3	3	3	702 (37)	−56.9	1.03 (0.02)	−0.27
4	2	1	1	2	2	1999 (145)	−66.0	1.43 (0.04)	−3.10
5	2	2	2	3	3	1167 (101)	−61.4	1.02 (0.00)	−0.15
6	2	3	3	1	1	1700 (118)	−64.6	1.02 (0.02)	−0.21
7	3	1	2	1	3	2348 (125)	−67.4	1.17 (0.06)	−1.40
8	3	2	3	2	1	2609 (128)	−68.3	1.03 (0.03)	−0.24
9	3	3	1	3	2	1618 (82)	−64.2	1.01 (0.00)	−0.12
10	1	1	3	3	2	869 (74)	−58.8	1.07 (0.01)	−0.62
11	1	2	1	1	3	540 (37)	−54.7	1.01 (0.00)	−0.09
12	1	3	2	2	1	955 (23)	−59.6	1.04 (0.00)	−0.35
13	2	1	2	3	1	2350 (132)	−67.4	1.27 (0.01)	−2.10
14	2	2	3	1	2	1786 (63)	−65.0	1.01 (0.00)	−0.05
15	2	3	1	2	3	1405 (79)	−63.0	1.03 (0.01)	−0.27
16	3	1	3	2	3	2080 (64)	−66.4	1.08 (0.01)	−0.67
17	3	2	1	3	1	1221 (80)	−61.7	1.02 (0.01)	−0.14
18	3	3	2	1	2	1422 (160)	−63.1	1.00 (0.00)	−0.04

y raw data (response variable); ( ) denotes standard deviation.

distribution and axial ratio were obtained by image analysis of SEM images (Rasband, 1997–2006). This method of size analysis was favored over dynamic light scattering and laser diffraction techniques because it allowed for an unbiased determination of the primary particle size, rather than that of the agglomerate. Nanoparticles have a high tendency to agglomerate in solution. The length was defined as the longest dimension of the particle passing through its geometric centre, while the width was the shortest dimension. Particle morphology was described by the axial ratio (i.e. ratio of length to width). In the case of a perfectly spherical particle, its longest dimension will be the same as its shortest dimension and the axial ratio will be '1'. To ensure the size distributions were representative of the powder, random samples were taken. Briefly, random sampling of the particles was carried out as follows: particle positioning was determined via the use of a 100-mesh transmission electron microscopy (TEM) grid (GCu100, ProSciTech, Australia) as the reference background (88 segments). A random list of the segments was generated by a random number generator (Minitab Inc., release 13, for Windows). At least 100 particles were measured for each sample from the random fields of view. All the experiments and measurements were performed in triplicate.

3. Results and discussion

Table 2 illustrates the structure of Taguchi's L_{18} orthogonal array, the respective measurement results and the corresponding S/N ratios. Tables 3 and 4 show the mean S/N ratio for each level of parameters (A–E) for the particle size and particle morphology, respectively. The effects of each factor are discussed in detail below. The parameter with the largest range was considered the critical factor affecting that particular response.

3.1. Particle morphology

There were four types of morphologies observed: (a) smooth spherical, (b) wrinkled, (c) mixed wrinkled and donut-shaped, and (d) chips and granules (Fig. 4). Smooth spherical BSA particles were obtained from formulations with added surfactant, while the other species (wrinkled, mixed wrinkled and donut-shaped, chips and granules) were obtained from surfactant-free ones. Tween 80, a non-ionic surfactant, was applied in the formulation as it is a commonly used excipient present in a number of protein-based pharmaceutical products. Furthermore, it has the added advantage of inhibiting protein aggregation (Kerwin et al., 1998; Wang et al., 2008). The addition of Tween 80 to the BSA solution altered the balance of surface-to-viscous forces so as to promote a smooth particle surface after spray drying (Adler et al., 2000). Previous reports have also shown that addition of surfactant to the formulation resulted in much smoother particle exteriors (Adler et al., 2000; Maa et al., 1997; Salama et al., 2009).

Table 3 shows that the morphology of the BSA particle was predominantly affected by the surfactant concentration (parameter B in the formulation (range 1.61). Fig. 5 shows the S/N response graph for the morphology of the particle, which was represented by the axial ratio. It could be observed from Table 2, that six out of the eighteen experimental runs (i.e. runs 1, 4, 7, 10, 13 and 16) had axial ratios deviating from unity (i.e. ≥1.05). These six runs shared a common ground, which was 0% surfactant concentration in the formulations. Addition of surfactant improved the sphericity of the particle, lowering the axial ratios to <1.05. Only a small amount of Tween 80 (i.e. 0.05%, w/v) was sufficient to reduce the morphology drastically from irregular to spherical. This observation was evident from the SEM images of runs 1 and 11 (Fig. 6) whereby the experimental conditions of both runs differed only by the amount of surfactant used and the inlet temperature. As inlet

Table 3
S/N response for axial ratio (dB).

Level	A	B	C	D	E
1	−0.66	−1.74	−1.04	−0.72	−0.93
2	−0.98	−0.13	−0.69	−0.79	−0.67
3	−0.43	−0.21	−0.34	−0.57	−0.48
Range	0.55	1.61	0.70	0.23	0.45
Rank	3	1	2	5	4

Letters (A–E) denote the experimental parameters.

Table 4
S/N response for particle size (dB).

Level	A	B	C	D	E
1	−57.78	−63.99	−61.25	−62.13	−63.51
2	−64.57	−61.41	−62.94	−63.67	−62.41
3	−65.19	−62.14	−63.35	−61.74	−61.62
Range	7.65	2.58	2.10	1.69	1.66
Rank	1	2	3	4	5

Letters (A–E) denote the experimental parameters.

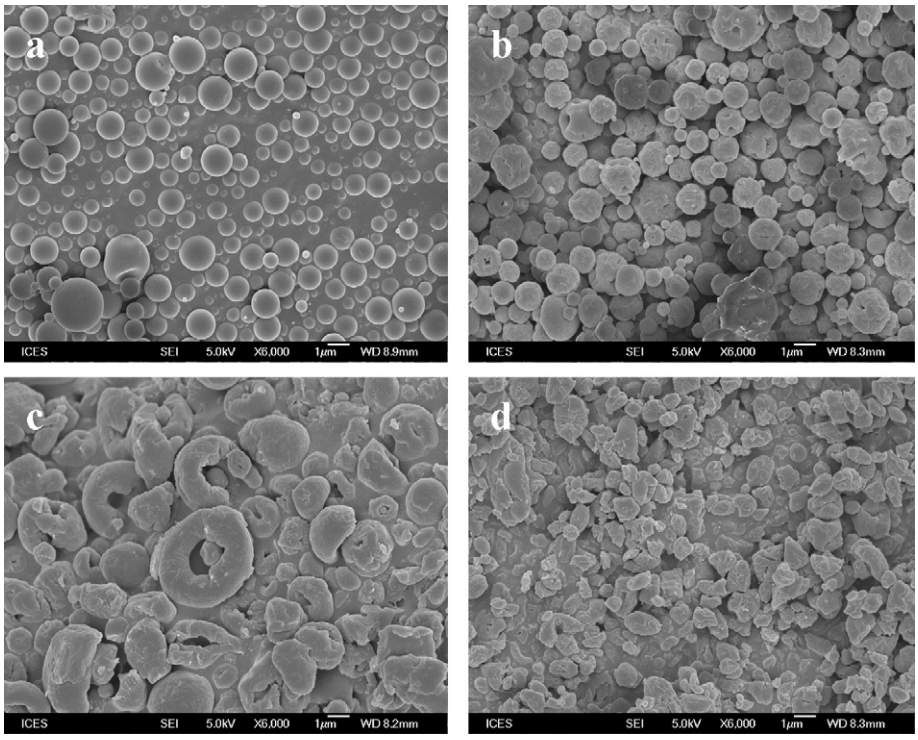

Fig. 4. FESEM images of spray-dried BSA particles with different morphologies: (a) smooth spherical, (b) wrinkled, (c) mixed wrinkled and donut-shaped, and (d) chips and granules.

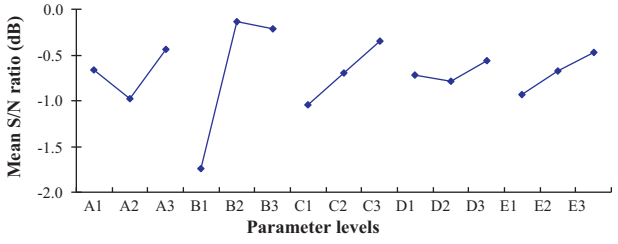

Fig. 5. S/N graph for axial ratio (particle morphology) response. Letters (A–E) denote the experimental parameters and numeric values denote the parameter levels.

temperature was found to have minimal influence (i.e. rank = 4) on the particle morphology (Fig. 5), the difference in morphology could be attributed mainly to the presence of the surfactant. However, increasing the concentration of Tween 80 from 0.05% (w/v) to 0.5% (w/v) gave no further improvements to the axial ratio. This could be due to saturation of the particle surface with surfactant molecules at the concentration of 0.05% (w/v). The presence of more surfactant molecules on the particle surface did not result in further reduction to the interfacial surface tension, which was a crucial factor in determining particle morphology.

The concentration of the protein solution (parameter C) was the next most important factor influencing the morphology of BSA particles (rank = 2, range = 0.70) (Table 3). SEM images (Fig. 7) from runs 1 and 10 could be used to clearly illustrate the effect of BSA solution concentration on the particle morphology. As both runs 1 and 10 had no added surfactant, the dominant variable on the particle morphology (i.e. surfactant concentration) was removed. Although the inlet temperature and nitrogen flow rate of both runs were different, the impact of these two parameters on the particle morphology was minimal (i.e. ranks 4 and 5, respectively). Therefore, the difference in morphology could be attributed mainly to the concentration of the protein solution. Particles obtained from run 1 (BSA concentration = 0.5%, w/v) were irregular while those from run 10 (BSA concentration = 2%, w/v) were more spherical. This observation clearly indicated that in the absence of the main dominating variable (i.e. surfactant concentration), the influence of BSA solution concentration on the surface morphology was more pronounced presumably due to BSA being slightly surface active

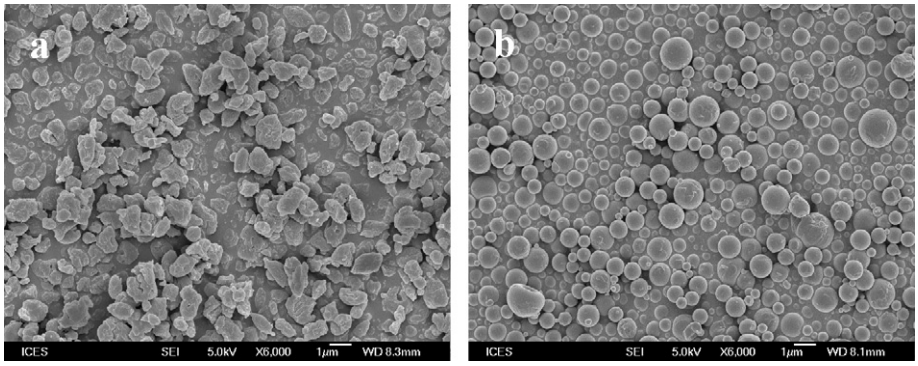

Fig. 6. FESEM images of (a) run 1 (0%, w/v Tween 80) and (b) run 11 (0.05%, w/v Tween 80), showing the effect of surfactant (Tween 80) on the sphericity of BSA particles.

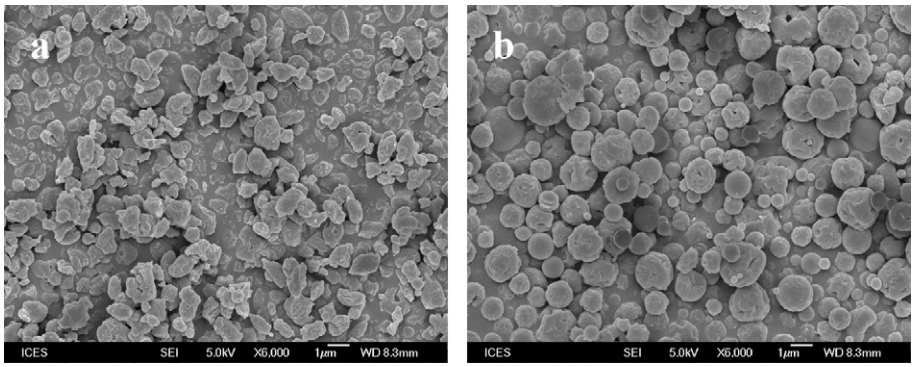

Fig. 7. FESEM images of (a) run 1 (0.5%, w/v BSA solution) and (b) run 10 (2%, w/v BSA solution), showing the effect of BSA solution concentration on the sphericity of BSA particles.

(Adler et al., 2000). This observation was in good agreement to a previous finding on a different spray drying system, whereby an increase to the feed solids concentration resulted in the formation of spherical particles (Langrish et al., 2006).

The effect of the mesh size on particle morphology was minimal (i.e. rank = 3), when compared to the contributions from the surfactant and protein concentrations. This could also be inferred by the equilateral 'V'-shaped response graphs whereby an incremental or decremental profile was not observed (Heng et al., 2009). Therefore, the spray mesh size, inlet temperature and nitrogen flow rate were found to have minimal influence on the BSA particle morphology. The importance of particle morphology to drug delivery cannot be over-emphasized. For example, in inhalation drug delivery, it is one of the important formulation factors influencing robust aerosol deposition (Crowder et al., 2002). Previously, surface corrugation had been found to improve the aerosol performance of BSA microparticles significantly (Adi et al., 2008; Chew et al., 2005). On the other hand, smooth round particles are also favored for ease of powder flow down a hopper. Therefore, the ability to tune the morphology of particles to suit the individual application would be highly beneficial to the pharmaceutical industry.

3.2. Geometric particle size

Table 4 shows that the spray mesh size (parameter A) had the greatest influence on the geometric particle size of BSA (range = 7.65). A decrease in the spray mesh size significantly reduced the particle size of BSA (Fig. 8). This parameter by far, outstrips the influence exerted by the other factors (i.e. surfactant concentration, BSA solution concentration, nitrogen flow rate and inlet temperature: range 1.66–2.58). It could be observed from Table 2, that six out of the eighteen experimental runs (i.e. runs 1, 2, 3, 10, 11 and 12) had particle sizes in the sub-micron range (<1 μm). These six runs shared a common ground, which was the use of the 4 μm spray mesh with varying levels set for the other parameters.

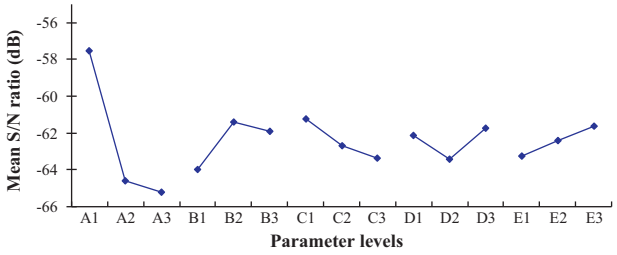

Fig. 8. S/N graph for particle size response. Letters (A–E) denote the experimental parameters and numeric values denote the parameter levels.

The results hence demonstrated the dominance of this factor over all the other set variables for particle size (i.e. rank 1). Fig. 9 illustrates the SEM images of the spray-drying runs that involved the 4.0 μm (i.e. run 2), 5.5 μm (i.e. run 5) and 7.0 μm (i.e. run 8) spray meshes, corresponding to droplet sizes of approximately 4.8 μm, 6.0 μm and 7.2 μm, respectively (Schmid et al., 2010). As expected, there was an obvious reduction of particle size with decreasing spray mesh size. Although these three runs varied in the protein concentration, nitrogen flow rate and inlet temperature, the impact of these variables on the size was minimal (ranks 3–5). The weak dependence of the particle size on the protein concentration is not surprising as the particle diameter is proportional to the cube root of the concentration (Kaerger and Price, 2004).

There is often a close correlation between the spray droplet size and the solid particle size after drying (Schmid et al., 2010). Therefore, factors affecting the droplet size would also have an effect on the solid particle size. Nozzle design, physical properties of feed, feed solids concentration and applied drying temperatures have all been reported to affect the droplet size of conventional spray dryers utilizing pneumatic air spray nozzles (Masters, 1976; Schmid et al., 2010). For the present study on the novel Nano Spray Dryer B-90, the BSA particle size was predominantly controlled by the spray mesh size. Although surfactant and protein concentrations were ranked as second and third, respectively, their influences were minimal in relation to the spray mesh size (i.e. ranges 2.10–2.58 versus range 7.65, Table 4). These findings were consistent with a recent study on the droplet size by Schmid et al. (2010), which found that the total solids concentration, viscosity and surface tension of the spray solution had very little impact on the eventual droplet size.

Nanoparticles offer a whole host of benefits to the pharmaceutical formulation, ranging from increased drug solubility and enhanced bioavailability to improved tissue targeting and decreased side-effects (Jia, 2005; Merisko-Liversidge et al., 2003). However, the production and collection of these nanoparticles in the spray-dried powder form has not been easy. Conventional spray dryers are more commonly designed for microparticles with yields in the range of 20–50% (Shoyele and Cawthome, 2006). Presently, the production of spray dried nanoparticles involves a two-step approach (micro-mixing and then conventional spray drying) that typically utilizes one or more surfactants to control the size (Chiou et al., 2008). The strength of the Nano Spray Dryer B-90 lies in its ability to regulate the size of particles down to the nanometre range directly from solution (i.e. one-step approach) and at high yields (70–90%).

Table 2 also showed that the median particle size of all the 18 runs were under 5 μm, which clearly demonstrated the suitability of the Nano Spray Dryer B90 for generating formulations aimed at inhalation drug delivery.

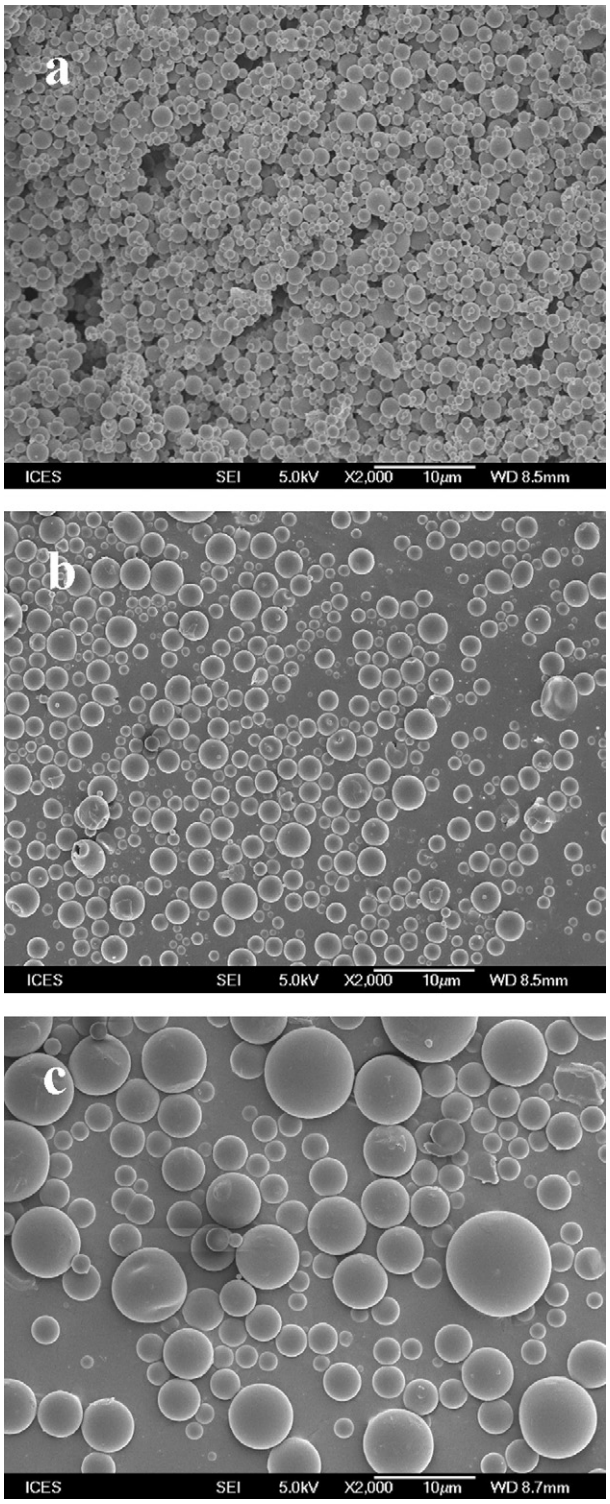

Fig. 9. FESEM images of (a) run 2 (4.0 μm spray mesh), (b) run 5 (5.5 μm spray mesh) and (c) run 8 (7.0 μm spray mesh), showing the effect of spray mesh size on the particle size of BSA particles.

3.3. Optimized conditions

Careful tuning of the various process and formulation parameters is vital to obtain particles of a desired size and morphology. In this work, smooth spherical BSA nanoparticles were desired to obtain discrete unaggregated particles. Optimum conditions were indicated by high S/N ratios. The greater the S/N ratio, the smaller

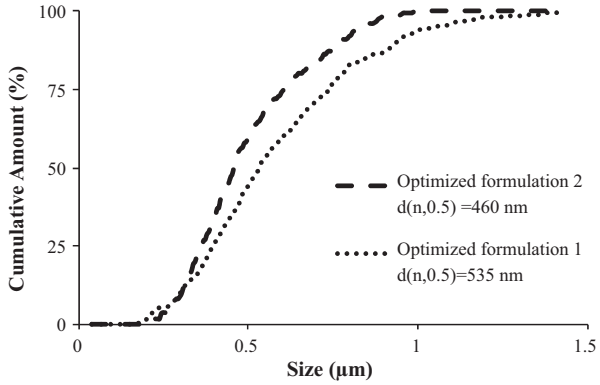

Fig. 10. Cumulative distribution for particle size of optimized formulation 1 and optimized formulation 2.

is the variance of particle size around the desired value. Therefore, based on the S/N response graph for particle size (Fig. 8), the optimal conditions were A at level 1, B at level 2, C at level 1, D at level 3 and E at level 3 (i.e. A1, B2, C1, D3, E3; optimized formulation 1). The suggested combination was very similar to run 11 in the Taguchi array, with the exception of the nitrogen flow rate (i.e. 90 L/min for run 11 and 120 L/min for optimized formulation 1). As the nitrogen flow rate was previously found to have minimal impact on the particle size, the suggested combination was likely to yield similar results to run 11. Run 11 was previously found to have the smallest median particle size among the 18 runs. When the suggested optimized run was carried out, indeed, the results were comparable to run 11. The median particle size was 535 ± 32 nm (Fig. 10) (compared to 540 ± 37 nm for run 11), while the product yield was $75 \pm 5\%$. As this formulation involved the addition of surfactant, the morphology was understandably smooth and spherical (Fig. 11a and b).

As there was no significant improvement to the particle size within the range studied, the formulation was re-optimized for further size reduction. Although the spray mesh size was previously identified to be the main parameter controlling the particle size and utilizing a smaller spray mesh would logically be the next approach, this option was not feasible as much smaller spray mesh sizes were not commercially available with the current setup. Due to the hardware constraints, the process parameters had to be manipulated instead. The only feasible parameter left to tune was the BSA solution concentration (minor parameter, rank 3), as the surfactant concentration was already at its specific optimum for both size and morphology.

Going with the slight trend shown in Fig. 8, a decreasing protein concentration favored a reduction in particle size. Therefore, the optimal conditions were now revised to a BSA solution concentration (parameter C) of 0.1% (w/v) (i.e. outside the studied range) (optimized formulation 2). The other parameters were the same as in optimized formulation 1. When the improved optimized run was carried out (i.e. optimized formulation 2), indeed, there was a decrease in the particle size from 535 ± 32 nm to 460 ± 10 nm (Fig. 10). The obtained nanoparticles were smooth and spherical (axial ratio = 1.03 ± 0.00) (Fig. 11c and d), narrowly distributed with a span of 1.03 ± 0.03, and had a high yield of $72 \pm 4\%$. The results thus showed the robustness of the Taguchi method in optimizing the size and morphology of BSA nanoparticles.

In this work, both optimized formulations were obtained in high yields (i.e. >70%), which clearly demonstrated the efficiency of the Nano Spray Dryer B-90's electrostatic particle collector. Even at high inlet temperatures of around 120 °C, a low outlet temperature was easily maintained. For example, at inlet temperatures of 80 °C, 100 °C and 120 °C, the range of outlet temperatures observed in this

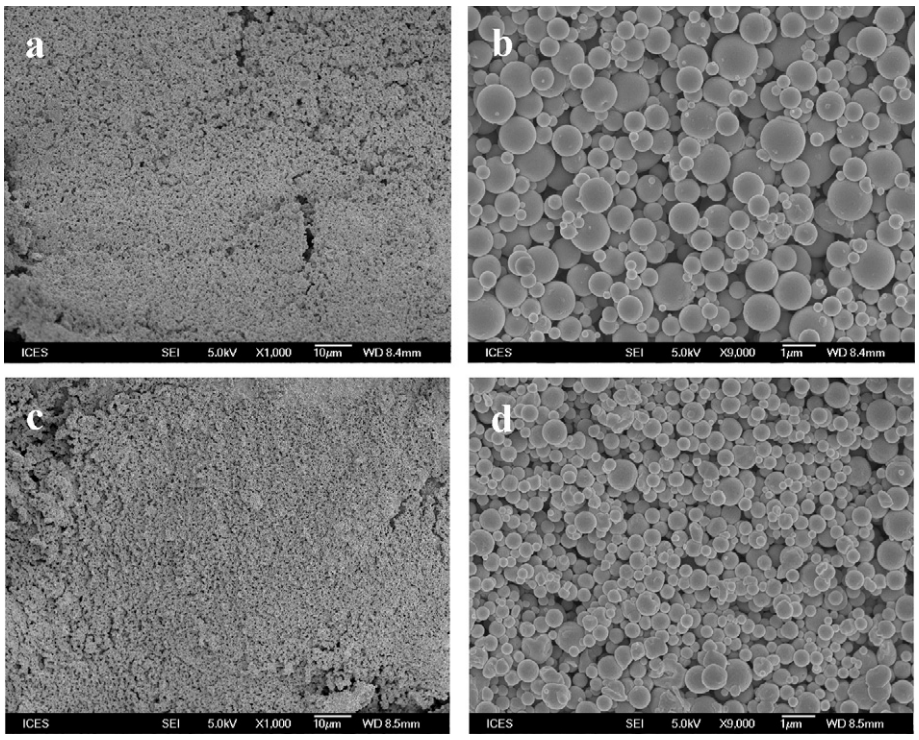

Fig. 11. FESEM images of the spray-dried BSA particles from (a) optimized formulation 1 and (b) optimized formulation 1 (close-up view); (c) optimized formulation 2 and (d) optimized formulation 2 (close-up view).

study were in the range of 36–40 °C, 42–45 °C and 51–55 °C, respectively. Clearly, these low outlet temperatures are highly favorable for the spray drying of temperature-sensitive peptides and proteins (Costantino et al., 1998). Therefore, the advent of the Nano Spray Dryer B-90 has indeed made spray drying of protein nanotherapeutics a reality.

4. Conclusions

Although spray-dried nanoparticles could be obtained via micro-mixing coupled with conventional spray drying approaches, the Nano Spray Dryer B-90 offers a novel one-step solution-based alternative at much higher yields. Via the Taguchi experimental design, it was found that the particle size and morphology of BSA nanoparticles were largely regulated by the spray mesh size and surfactant concentration, respectively. Optimized production of smooth spherical nanoparticles (median size: 460 ± 10 nm, axial ratio: 1.03 ± 0.00, span 1.03 ± 0.03, yield: $72 \pm 4\%$) was achieved using the 4 μm spray mesh at BSA concentration of 0.1% (w/v), surfactant concentration of 0.05% (w/v), drying flow rate of 150 L/min and inlet temperature of 120 °C. The results obtained in this study will no doubt be useful to formulation scientists contemplating protein nanoparticles in their formulations.

Acknowledgements

This work was supported by the Science and Engineering Research Council of A*STAR (Agency for Science, Technology and Research), Singapore (grant no. ICES/09-122A02). We are grateful to Miss Tan Li Teng, Mr. Ng Jun Wei and Miss Shirley Yap for their assistance in the experiments. We also thank Dr. Cordin Arpagaus (BÜCHI Labortechnik AG) for the fruitful discussion and Dr. Philip Kwok (The University of Sydney) for the helpful advice.

References

Adi, S., Adi, H., Tang, P., Traini, D., Chan, H.K., Young, P.M., 2008. Micro-particle corrugation, adhesion and inhalation aerosol efficiency. European Journal of Pharmaceutical Sciences 35, 12–18.

Adler, M., Unger, M., Lee, G., 2000. Surface composition of spray-dried particles of bovine serum albumin/trehalose/surfactant. Pharmaceutical Research 17, 863–870.

Broadhead, J., Rouan, S.K.E., Rhodes, C.T., 1992. The spray drying of pharmaceuticals. Drug Development and Industrial Pharmacy 18, 1169–1206.

BÜCHI Labortechnik AG, 2009. Switzerland Brochure Nano Spray Dryer B-90. Flawil, Switzerland.

Cal, K., Sollohub, K., 2010. Spray drying technique. I: hardware and process parameters. Journal of Pharmaceutical Sciences 99, 575–586.

Chan, H.K., Clark, A., Gonda, I., Mumenthaler, M., Hsu, C., 1997. Spray dried powders and powder blends of recombinant human deoxyribonuclease (rhDNase) for aerosol delivery. Pharmaceutical Research 14, 431–437.

Chew, N.Y.K., Tang, P., Chan, H.K., Raper, J.A., 2005. How much particle surface corrugation is sufficient to improve aerosol performance of powders? Pharmaceutical Research 22, 148–152.

Chiou, H., Chan, H.K., Heng, D., Prud'homme, R.K., Raper, J.A., 2008. A novel production method for inhalable cyclosporine A powders by confined liquid impinging jet precipitation. Journal of Aerosol Science 39, 500–509.

Cleland, J.L., Daugherty, A., Mrsny, R., 2001. Emerging protein delivery methods. Current Opinion in Biotechnology 12, 212–219.

Coppi, G., Iannuccelli, V., Bernabei, M.T., Cameroni, R., 2002. Alginate microparticles for enzyme peroral administration. International Journal of Pharmaceutics 242, 263–266.

Costantino, H.R., Andya, J.D., Nguyen, P.A., Dasovich, N., Sweeney, T.D., Shire, S.J., et al., 1998. Effect of mannitol crystallization on the stability and aerosol performance of a spray-dried pharmaceutical protein, recombinant humanized anti-IgE monoclonal antibody. Journal of Pharmaceutical Sciences 87, 1406–1411.

Crowder, T.M, Rosati, J.A., Schroeter, J.D., Hickey, A.J., Martonen, T.B., 2002. Fundamental effects of particle morphology on lung delivery: predictions of Stokes' law and the particular relevance to dry powder inhaler formulation and development. Pharmaceutical Research 19, 239–245.

Diemunsch, A.M., Pabst, J.Y., Constant, C., Mathis, C., Stamm, A., 1993. Tablet formulation—Taguchi, Genichi approach. Drug Development and Industrial Pharmacy 19, 1461–1477.

Ellis-Behnke, R.G., Liang, Y.X., You, S.W., Tay, D.K.C., Zhang, S.G., So, K.F., et al., 2006. Nano neuro knitting: peptide nanofiber scaffold for brain repair and axon regeneration with functional return of vision. Proceedings of the National Academy of Sciences of the United States of America 103, 5054–5059.

Ghadiri, M.R., Granja, J.R., Buehler, L.K., 1994. Artificial transmembrane ion channels from self-assembling peptide nanotubes. Nature 369, 301–304.

Heng, D., Cutler, D.J., Chan, H.K., Yun, J., Raper, J.A., 2008. What is a suitable dissolution method for drug nanoparticles? Pharmaceutical Research 25, 1696–1701.
Heng, D., Ogawa, K., Cutler, D.J., Chan, H.K., Raper, J.A., Ye, L., et al., 2009. Pure drug nanoparticles in tablets: what are the dissolution limitations? Journal of Nanoparticle Research 12, 1743–1754.
Jia, L., 2005. Nanoparticle formulation increases oral bioavailability of poorly soluble drugs: approaches, experimental evidences and theory. Current Nanoscience 1, 237–243.
Kaerger, J.S., Price, R., 2004. Processing of spherical crystalline particles via a novel solution atomization and crystallization by sonication (SAXS) technique. Pharmaceutical Research 21, 372–381.
Kaye, R.S., Purewal, T.S., Alpar, O.H., 2009. Development and testing of particulate formulations for the nasal delivery of antibodies. Journal of Controlled Release 135, 127–135.
Kerwin, B.A., Heller, M.C., Levin, S.H., Randolph, T.W., 1998. Effects of Tween 80 and sucrose on acute short-term stability and long-term storage at −20 °C of a recombinant hemoglobin. Journal of Pharmaceutical Sciences 87, 1062–1068.
Kim, K.D., Choi, D.W., Choa, Y.H., Kim, H.T., 2007. Optimization of parameters for the synthesis of zinc oxide nanoparticles by Taguchi robust design method. Colloids and Surfaces A: Physicochemical and Engineering Aspects 311, 170–173.
Koster, V.S., Kuks, P.F.M., Lange, R., Talsma, H., 1996. Particle size in parenteral fat emulsions, what are the true limitations? International Journal of Pharmaceutics 134, 235–238.
Langrish, T.A.G., Marquez, N., Kota, K., 2006. An investigation and quantitative assessment of particle shape in milk powders from a laboratory-scale spray dryer. Drying Technology 24, 1619–1630.
Larry, R.B., 2005. Commercial challenges of protein drug delivery. Expert Opinion on Drug Delivery 2, 29–42.
Lee, S.H., Zhang, Z.P., Feng, S.S., 2007. Nanoparticles of poly(lactide)–tocopheryl polyethylene glycol succinate (PLA–TPGS) copolymers for protein drug delivery. Biomaterials 28, 2041–2050.
Maa, Y., Costantino, H.R., Nguyen, P.A., Hsu, C.C., 1997. The effect of operating and formulation variables on the morphology of spray-dried protein particles. Pharmaceutical Development and Technology 2, 213–223.
Masters, K., 1976. Spray Drying. Wiley, London.
Merisko-Liversidge, E., Liversidge, G.G., Cooper, E.R., 2003. Nanosizing: a formulation approach for poorly-water-soluble compounds. European Journal of Pharmaceutical Sciences 18, 113–120.
Merisko-Liversidge, E., McGurk, S.L., Liversidge, G.G., 2004. Insulin nanoparticles: a novel formulation approach for poorly water soluble Zn-insulin. Pharmaceutical Research 21, 1545–1553.
Mosen, K., Backstrom, K., Thalberg, K., Schaefer, T., Kristensen, H.G., Axelsson, A., 2004. Particle formation and capture during spray drying of inhalable particles. Pharmaceutical Development and Technology 9, 409–417.
Muller, R.H., Junghanns, J.A.H., 2006. Drug nanocrystals/nanosuspensions for the delivery of poorly soluble drugs. In: Torchilin, V.P. (Ed.), Nanoparticulates as Drug Carriers. Imperial College Press, London, pp. 308–309.
Noyes, A., Whitney, W.J., 1897. The rate of solution of solid substances in their own solutions. Journal of the American Chemical Society 19, 930–934.
Palmieri, G.F., Wehrle, P., 1997. Evaluation of ethylcellulose-coated pellets optimized using the approach of Taguchi. Drug Development and Industrial Pharmacy 23, 1069–1077.
Peace, G.S., 1993. Taguchi Methods. A hands-on Approach to Quality Engineering. Addison–Wesley, Massachusetts.
Rasband, W. S., 1997–2006. ImageJ (http://rsb.info.nih.gov/ij/). U.S. National Institutes of Health, Bethesda, MD, USA.
Salama, R.O., Traini, D., Chan, H.K., Sung, A., Ammit, A.J., Young, P.M., 2009. Preparation and evaluation of controlled release microparticles for respiratory protein therapy. Journal of Pharmaceutical Sciences 98, 2709–2717.
Schmid, K., Arpagaus, C., Friess, W., 2010. Evaluation of the Nano Spray Dryer B-90 for pharmaceutical applications. Pharmaceutical Development and Technology Early Online, 1–8.
Shaji, J., Patole, V., 2008. Protein and peptide drug delivery: oral approaches. Indian Journal of Pharmaceutical Sciences 70, 269–277.
Shoyele, S.A., Cawthome, S., 2006. Particle engineering techniques for inhaled biopharmaceuticals. Advanced Drug Delivery Reviews 58, 1009–1029.
Souto, E.B., Muller, R.H., 2008. Cosmetic features and applications of lipid nanoparticles (SLN®, NLC®). International Journal of Cosmetic Science 30, 157–165.
Taguchi, G., 1986. Introduction to Quality Engineering: Designing Quality into Products and Processes. UNIPUB/Kraus, New York.
Wang, W., Wang, Y.J., Wang, D.Q., 2008. Dual effects of Tween 80 on protein stability. International Journal of Pharmaceutics 347, 31–38.
Yang, K., Teo, E.C., Fuss, F.K., 2007. Application of Taguchi method in optimization of cervical ring cage. Journal of Biomechanics 40, 3251–3256.